# External sensorless adaptive chatter avoidance in NC machining by applying disturbance observer using high resolution linear encoder

Takaki Shimoda[1], Hiroshi Fujimoto[1], Norihiro Kumagai[2] and Yuki Terada[2]

*Abstract*— **The productivity of numerical control (NC) machining is highly limited by the occurrence of chatter vibration. Chatter stability analyses are widely studied to predict chatter vibration. However, these analyses often fail to provide reliable prediction results because the parameters in the vibration model are sensitive to identification errors, mechanical deterioration and thermal changes. On the other hand, to implement robust avoidance of chatter vibration to process changes, additional external sensors have been used, *e.g.* accelerometers and force sensors. However, this results in increase in cost and decrease in rigidity of the installation site. Meanwhile in recent years, there has been a growing trend toward including a high resolution linear encoder as a standard equipment for a NC machine. In this paper, by applying a disturbance observer using a high resolution linear encoder, an external sensorless adaptive spindle speed selection method is proposed for the robust chatter avoidance. The proposed method is verified by experimental studies on a NC end milling machine.**

## I. INTRODUCTION

Chatter vibration highly limits both the accuracy and the material removal rate of NC machining. Moreover, its strong vibration often results in a tool breakage [1], [2]. There are two reasons for the occurrence of chatter vibration: one reason is regenerative variation of the chip thickness called regenerative effect [3] and the other reason is external disturbances [4]. Chatter vibration caused by the regenerative effect is called self-excited chatter vibration, which is the main cause of the chatter vibration problems because the regenerative effect makes machining unstable [3].

Inefficient measures, *e.g.* limiting the depth of cut, are often taken to suppress chatter vibration in general, which reduces the productivity of the machining. Hence, there have been many works aiming to avoid chatter vibration without impairing the productivity. Particularly, many works have been conducted to obtain a precise vibration model of a chatter phenomenon [1], [3]–[6]. The aim of these works is to identify conditions where self-excited chatter vibration will not occur by conducting stability analyses. However, these analyses cannot always be applied to actual commercial machining because of identification errors, mechanical deterioration, and thermal changes [6]–[9].

Contrary to these *out-of-process* approaches, *in-process* approaches have been proposed that adaptively changes the rotational speed of the spindle using information during the machining process to avoid chatter vibration [6]–[9]. The in-process methods are robust to modeling uncertainty and changing process conditions.

However, most of in-process approaches use external sensors, *e.g.* accelerometers and force sensors [6], [8]. As a result, the cost increases and the rigidity in the installation site decreases. In order to solve these problems, a few works on sensorless detection and avoidance of chatter vibration have been conducted applying a disturbance observer using the spindle encoder [7], [9]. However, since the accuracy of the spindle encoder is not necessarily required high only for spindle speed control [10], it is difficult to assume that the spindle encoder resolution is high enough to observe high frequency chatter vibration.

Meanwhile in recent years, there is a trend to equip a high resolution linear encoder for precise NC machining [11]. In this paper, using a high resolution linear encoder, an external sensorless chatter frequency estimation method is proposed by applying a disturbance observer. In addition, a sensorless adaptive chatter avoidance is proposed based on the proposed frequency estimation method, which is robust to the modeling errors of the vibration model. The proposed chatter avoidance method is provided in section III. Simulation in section IV and experimental studies in section V on a NC end milling machine verify the proposed chatter avoidance method.

## II. Dynamics of milling and chatter stability analysis

This paper deals with two-degrees-of-freedom (2DOF) milling. Fig. 1a shows the mechanical 2DOF milling model. The equation of motion of 2DOF milling is given by [5]

$$\boldsymbol{M}\ddot{\boldsymbol{q}}(t) + \boldsymbol{C}\dot{\boldsymbol{q}}(t) + \boldsymbol{K}\boldsymbol{q}(t) = \boldsymbol{F}_{\mathrm{c}}(t), \tag{1}$$

where

$$\boldsymbol{q}(t) = \begin{bmatrix} x(t) & y(t) \end{bmatrix}^T, \boldsymbol{F}_{\mathrm{c}}(t) = \begin{bmatrix} F_x(t) & F_y(t) \end{bmatrix}^T. \tag{2}$$

Here $\boldsymbol{q}$ is the position of the tool. $\boldsymbol{F}_{\mathrm{c}}$ is the cutting force vector and represents the force applied to the tool. $\boldsymbol{M}, \boldsymbol{C}, \boldsymbol{K}$ are equivalent mass, viscosity, and stiffness matrix, respectively.

The chip thickness $\boldsymbol{h}$ consists of the static chip thickness $\boldsymbol{h}_0$ and the dynamic chip thickness $\boldsymbol{h}_{\mathrm{d}}$, given by (3) [3]. $\boldsymbol{h}_0$ is the feed per tooth and $\boldsymbol{h}_{\mathrm{d}}$ is the regenerative variation of chip thickness due to the tool position variation between previous and current tooth path.

$$\boldsymbol{h}(t) \quad = \quad \boldsymbol{h}_0 - \boldsymbol{h}_{\mathrm{d}}(t), \tag{3}$$

where

$$\boldsymbol{h}_{\mathrm{d}}(t) \quad = \quad \boldsymbol{q}(t) - \boldsymbol{q}(t - \tau(t)). \tag{4}$$

[1] The University of Tokyo, 5-1-5, Kashiwanoha, Kashiwa 277-8561, Chiba, Japan. shimoda16@hflab.k.u-tokyo.ac.jp, fujimoto@k.u-tokyo.ac.jp

[2] DMG MORI CO., LTD, 362, Idono, Yamatokoriyama 639-1183, Nara, Japan. {yk-terada, no-kumagai}@dmgmori.co.jp

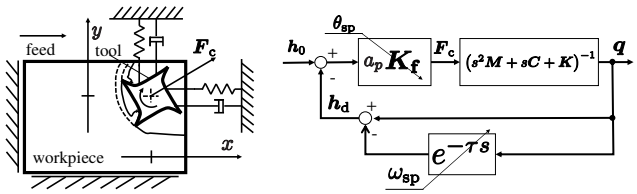


(a) Mechanical 2DOF milling model. (b) Block diagram of 2DOF milling.

Fig. 1: 2DOF milling.

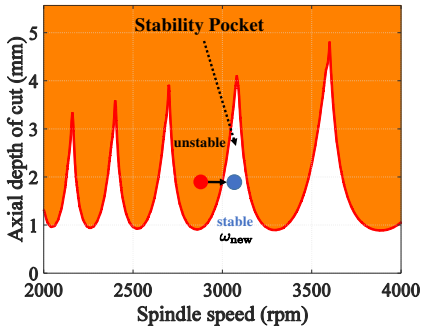


Fig. 2: An example of a stability lobe diagram. Colored area represents unstable cutting condition.

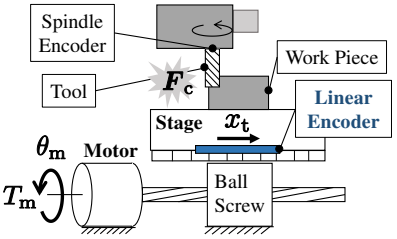


Fig. 3: NC machining table (ball-screw-driven) with a linear encoder.

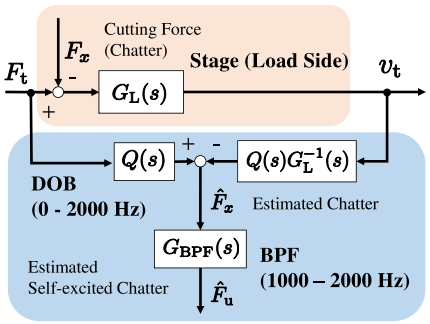


Fig. 4: Estimation of self-excited chatter $\hat{F}_u$ via a stage disturbance observer with a band-pass filter for the stage.

Here $\tau(t)$ is the regenerative delay between current and previous tooth path, which satisfies [4]

$$\int_{t-\tau(t)}^{t} \omega_{sp}(t)dt = \frac{2\pi}{q}, \tag{5}$$

where $q$ is the number of teeth of the tool. The cutting force vector is given by (6) as the total sum of the forces applied to each tooth [4], [5].

$$\boldsymbol{F}_c(t) = a_p \boldsymbol{K}_f(t)\boldsymbol{h}(t), \tag{6}$$

where

$$\boldsymbol{K}_f(t) = \sum_{j=1}^{q} g_j(t) \begin{bmatrix} \cos(\phi_j(t)) & -\sin(\phi_j(t)) \\ \sin(\phi_j(t)) & \cos(\phi_j(t)) \end{bmatrix}^{-1} \begin{bmatrix} K_t \\ K_r \end{bmatrix} \cdot \begin{bmatrix} \sin(\phi_j(t)) & \cos(\phi_j(t)) \end{bmatrix}. \tag{7}$$

Here $a_p$ is the axial depth of cut. $K_t$ and $K_r$ are the cutting force coefficients in the tangential and the normal direction, respectively. $g_j(t)$ is a screen function, which is 1 when the $j$-th tooth is in cut otherwise 0. $\phi_j(t)$ is the angle of the $j$ th tooth and $\omega_{sp}$ is the spindle velocity.

Fig.1b shows a block diagram of 2DOF milling, where $\theta_{sp}$ represents the angle of the spindle. Since there is the internal delayed feedback in the plant, if the depth of cut is taken deeply, the system becomes unstable and therefore the strong vibration, which is self-excited chatter vibration, results [1]. On the other hand, the vibration due to external disturbances is called forced chatter vibration [8].

Based on the above model of chatter vibration, methods to analytically identify unstable conditions have been studied [1], [3], [5]. A graph showing the stability boundary, with the spindle speed on the horizontal axis and the depth of cut on the vertical axis, is called a stability lobe diagram. A stability lobe diagram by the semi-discretization method [4], [5] is shown in Fig. 2. It is possible to analyze chatter phenomenon by this kind of analysis; however, the prediction accuracy is often not high enough due to modeling errors [7].

On the other hand, if it is possible to estimate the chatter frequency in real time, it is also possible to avoid chatter vibration robustly to modeling errors by selecting the new stable spindle velocity $\omega_{new}$ under a stable region in a stability lobe called stability pocket as shown in Fig. 2 [8].

## III. External sensorless adaptive chatter avoidance

In a conventional in-process chatter avoidance method, external sensors such as accelerometers are used to estimate the frequency of self-excited chatter vibration [8]. In this section, however, external sensorless method to avoid self-excited chatter vibration by spindle speed selection is proposed.

### *A. Estimation of self-excited chatter disturbance by using stage disturbance observer and band pass filter*

The proposed method estimates the self-excited chatter frequency by estimating the cutting force disturbance applied to the stage in the feed ($x$ in this paper) direction. The stage is equipped with the linear encoder on the load side as shown in Fig. 3. The relation among the driving side motor angular velocity $\omega_m$, the stage velocity $v_t$, the driving side torque $T_m$, and the cutting force disturbance $F_x$ applied to the stage can be described by (8) [12]. The stage velocity is obtained by the difference of the linear encoder position information.

$$\begin{bmatrix} \omega_m \\ v_t \end{bmatrix} = \begin{bmatrix} G_M(s) & G_{12}(s) \\ G_{21}(s) & G_L(s) \end{bmatrix} \begin{bmatrix} T_m \\ -F_x \end{bmatrix}, \tag{8}$$

where $G_{\mathrm{M}}(s), G_{12}(s), G_{21}(s)$ and $G_{\mathrm{L}}(s)$ are transfer functions.

By applying the disturbance observer (DOB) as shown in Fig. 4, the estimated cutting force $\hat{F}_{\mathrm{x}}$ is given by (9) from (8) if the modeling error is neglected [13].

$$\hat{F}_{\mathrm{x}} = Q(s)\left(F_{\mathrm{t}} - G_{\mathrm{L}}^{-1}(s)v_{\mathrm{t}}\right), \tag{9}$$

where

$$F_{\mathrm{t}} = \frac{G_{21}(s)}{G_{\mathrm{L}}(s)}T_{\mathrm{m}}. \tag{10}$$

Here $Q(s)$ is a low pass filter (LPF) designed so as to contain the frequency component of self-excited chatter vibration.

Since chatter vibration consists of forced and self-excited chatter vibration, the cutting force disturbance $F_x$ can be described as follows:

$$F_{\mathrm{x}} = F_{\mathrm{p}} + F_{\mathrm{u}}, \tag{11}$$

where $F_{\mathrm{p}}, F_{\mathrm{u}}$ are the components of forced and self-excited chatter vibration, respectively.

In general, the peak frequency of forced chatter vibration is within only a few hundred Hertz or less, whereas that of self excited-chatter vibration is exceeding 1000 Hz [9]. Therefore, only self-excited chatter signal can be extracted from chatter vibration signal by designing a band pass filter (BPF) $G_{\mathrm{BPF}}(s)$ which includes the peak frequency of self-exciting chatter vibration and does not include that of forced chatter vibration. Hence, the estimated self-excited chatter vibration component $\hat{F}_{\mathrm{u}}$ of the estimated cutting force $\hat{F}_{\mathrm{x}}$ is obtained as follows:

$$\hat{F}_{\mathrm{u}} = G_{\mathrm{BPF}}(s)\hat{F}_{\mathrm{x}}. \tag{12}$$

The bandwidth of $T_{\mathrm{m}}$ is limited by the stage velocity control system. In general, the bandwidth is tens of Hertz and is designed not to excite high frequency mechanical resonances [12]. Therefore, $G_{\mathrm{BPF}}(s)Q(s)F_{\mathrm{t}}$ filtered by the BPF is considered to be negligible since the cutoff frequency of the BPF is exceeding several hundred Hertz in general. Hence $\hat{F}_{\mathrm{u}}$ can be computed as

$$\hat{F}_{\mathrm{u}} = -G_{\mathrm{BPF}}(s)Q(s)G_{\mathrm{L}}^{-1}(s)v_{\mathrm{t}}. \tag{13}$$

In this paper, it is assumed that the peak frequency of self-excited chatter vibration exists between 1000 and 2000 Hz. Therefore the cutoff frequency of LPF $Q(s)$ is designed to 2000 Hz, and the bandpass frequency of BPF $G_{\mathrm{BPF}}(s)$ is designed to 1000 to 2000 Hz.

### *B. Adaptive estimation of self-excited chatter frequency using Kalman filter*

Assuming that the model of self-excited chatter is the time-variant autoregressive model whose system is excited by zero-mean white Gaussian noise $e[i]$, $F_{\mathrm{u}}$ is given by [8]

$$F_{\mathrm{u}}[i] = \frac{1}{D[z]}e[i], \tag{14}$$

where

$$D[z] = 1 + \sum_{n=1}^{N_{\mathrm{d}}} d_n z^{-n}. \tag{15}$$

Here the sequence $F_{\mathrm{u}}[i] = F_{\mathrm{u}}(it_{\mathrm{s}})$ $(i = 0, 1, 2...)$ is the digital representation of its continuous signal, where $t_{\mathrm{s}}$ is the sampling period. $\frac{1}{D[z]}$ is a transfer function which represents self-excited chatter and $N_{\mathrm{d}}$ is the number of its poles. Furthermore, a parameter vector $\boldsymbol{\theta}_{\mathrm{u}}[i]$ for $D[z]$ is defined by

$$\boldsymbol{\theta}_{\mathrm{u}}[i] = \begin{bmatrix} d_1 & d_2 & ... & d_{N_{\mathrm{d}}} \end{bmatrix}^T. \tag{16}$$

The state space model of the true parameter vector $\overline{\boldsymbol{\theta}}_{\mathrm{u}}$ can be described by (17), (18) derived from (14).

$$\overline{\boldsymbol{\theta}}_{\mathrm{u}}[i+1] = \overline{\boldsymbol{\theta}}_{\mathrm{u}}[i] + \boldsymbol{v}[i], \tag{17}$$

$$F_{\mathrm{u}}[i] = \boldsymbol{\phi}_{\mathrm{u}}^T[i]\overline{\boldsymbol{\theta}}_{\mathrm{u}}[i] + w[i], \tag{18}$$

where

$$\boldsymbol{\phi}_{\mathrm{u}}[i] = \begin{bmatrix} -F_{\mathrm{u}}[i-1] & \cdots & -F_{\mathrm{u}}[i-N_{\mathrm{d}}] \end{bmatrix}^T. \tag{19}$$

Here $\boldsymbol{v}[i] \sim \mathcal{N}(0, \boldsymbol{R}_v)$ and $w[i] \sim \mathcal{N}(0, R_w)$ are white Gaussian noises uncorrelated with each other and with the initial state vector of $\overline{\boldsymbol{\theta}}_{\mathrm{u}}$. From (17) and (18), the parameter vector $\boldsymbol{\theta}_{\mathrm{u}}$ is estimated in step $i > 0$ by the Kalman filter as follows [8]:

$$\boldsymbol{\theta}_{\mathrm{u}}[i+1] = \boldsymbol{\theta}_{\mathrm{u}}[i] + \boldsymbol{g}[i](\hat{F}_{\mathrm{u}}[i] - \boldsymbol{\phi}_{\mathrm{u}}^T[i]\boldsymbol{\theta}_{\mathrm{u}}[i]), \tag{20}$$

where

$$\boldsymbol{g}[i] = \frac{(\boldsymbol{P}[i-1] + \boldsymbol{R}_v[i])\boldsymbol{\phi}_{\mathrm{u}}[i]}{\boldsymbol{\phi}_{\mathrm{u}}^T[i](\boldsymbol{P}[i-1] + \boldsymbol{R}_v[i])\boldsymbol{\phi}_{\mathrm{u}}[i] + R_w[i]}, \tag{21}$$

$$\boldsymbol{P}[i] = (\boldsymbol{I} - \boldsymbol{g}[i]\boldsymbol{\phi}_{\mathrm{u}}^T[i])(\boldsymbol{P}[i-1] + \boldsymbol{R}_v[i]). \tag{22}$$

Here $\boldsymbol{P}[i]$ is the error covariance matrix and $\boldsymbol{g}[i]$ is the Kalman gain matrix whose initial value is zero.

The dominant self-excited chatter frequency $f_{\mathrm{chat}}[i]$ is calculated for each step $i$ as follows:

$$f_{\mathrm{chat}}[i] = \mathrm{Im}\left(\frac{\ln(\alpha)}{2\pi t_{\mathrm{s}}}\right), \tag{23}$$

where $\alpha$ is the dominant root of the estimated $\frac{1}{D[z]}$ .

### *C. In-process chatter avoidance by spindle speed selection*

Using the estimated dominant chatter frequency $f_{\mathrm{chat}}$ in (23), the self-excited chatter avoidance method by adjusting a spindle speed to a stable speed [8] is discussed below.

$f_{\mathrm{chat}}$ is related to the tooth-passing excitation frequency $f_{\mathrm{TPE}} \equiv q\omega_{\mathrm{sp}}/(2\pi)$, which can be described by [8]

$$\frac{f_{\mathrm{chat}}[i]}{f_{\mathrm{TPE}}[i]} = \rho + \frac{\epsilon}{2\pi}, \tag{24}$$

where $\rho$ is the lobe number and $\epsilon$ is the phase difference between the tooth passing frequency and the dominant self-excited chatter. Since the cutting condition when $\epsilon = 0$ locally maximizes the stability [8], the stable spindle speed $\omega_{\mathrm{new}}$ can be derived by calculating $\epsilon = 0$ as follows:

$$\rho_{\mathrm{new}}[i] = \mathrm{round}\left(\frac{f_{\mathrm{chat}}[i]}{f_{\mathrm{TPE}}[i]}\right), \tag{25}$$

$$\omega_{\mathrm{new}}[i] = \frac{2\pi f_{\mathrm{chat}}[i]}{\rho_{\mathrm{new}}[i]q}, \tag{26}$$

where $\omega_{\mathrm{new}}$ is the stable spindle speed under the stability pocket and $\rho_{\mathrm{new}}$ is its lobe number. round$(\cdot)$ is a rounding-off function. By rounding off, the spindle speed under the

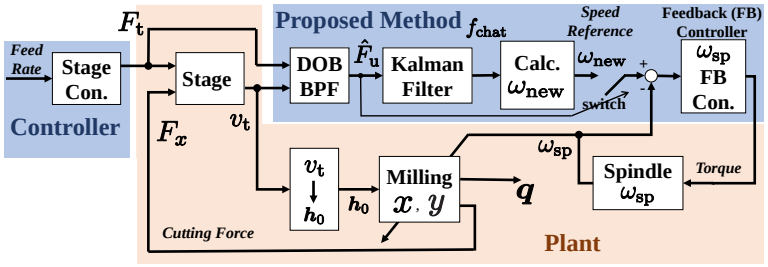


Fig. 5: Proposed external sensorless adaptive chatter avoidance. Con. denotes a controller.

TABLE I: Parameters in simulation and experimental studies.

(a) Mechanical.

| Symbol | |
|---|---|
| $\boldsymbol{M}$ | 0.40 $\boldsymbol{I}$ (kg) |
| $\boldsymbol{C}$ | 83.0 $\boldsymbol{I}$ (Ns m$^{-1}$) |
| $\boldsymbol{K}$ | 30.1 $\boldsymbol{I}$ (MN m$^{-1}$) |
| $K_t$ | 0.980 (GPa) |
| $K_r$ | 0.294 (GPa) |
| $q$ | 4 |
| Stage mass | 273 (kg) |

(b) Adaptive filter.

| Symbol | |
|---|---|
| $t_s$ | 250 ($\mu$s) |
| $N_d$ | 2 |
| $\boldsymbol{R}_v$ | $10^{-6}$ $\boldsymbol{I}$ |
| $R_w$ | 0.3 |
| $\boldsymbol{P}$ [0] | $10^3$ $\boldsymbol{I}$ |
| $\sigma_{th}$ | 10000 (N$^2$) |

(c) Machining condition

| Description | |
|---|---|
| Axial depth of cut $a_p$ | 3.5 (mm) |
| Radial depth of cut | 2 (mm) |
| Diameter of tool | 12 (mm) |
| Stage feed velocity | 0.5 (mm s$^{-1}$) |

nearest stability pocket can be obtained. Thus, this method enables automatically selecting the stable speed [8]. This stabilizing effect can be seen from the fact that the dynamic chip thickness $\boldsymbol{h}_d$ at the dominant chatter frequency $f_{chat}$ is 0 when this method is applied, as proven in (27) below. When (26) is applied and the spindle speed is in a steady state, $\boldsymbol{h}_d$ at the frequency $f_{chat}$ is given by (27) from (4) and (5).

$$\begin{aligned} \boldsymbol{h}_d|_{s=j2\pi f_{chat}} &= (1-e^{-\tau s})\boldsymbol{q}|_{s=j2\pi f_{chat}} \\ &= (1-e^{-j2\pi\rho_{new}})\boldsymbol{q} \quad \left(\because \tau = \frac{2\pi}{q\omega_{new}}\right) \\ &= \boldsymbol{0} \ (\because \rho_{new} \in \mathbb{N}). \end{aligned} \tag{27}$$

(27) shows that regenerative variation of chip thickness is removed at the frequency $f_{chat}$ when $\omega_{sp} = \omega_{new}$ and thereby that self-excited chatter vibration is suppressed.

Fig. 5 shows the proposed external sensorless adaptive chatter avoidance method. The proposed method starts when estimated power of self-excited chatter $\hat{F}_u^2$ exceeds a given threshold $\sigma_{th}$.

## IV. Simulation Results

Table 1 shows parameters of the milling and the adaptive filter. The bandwidths of the stage and the spindle velocity control are designed at 40 and 80 Hz, respectively. In the simulation, cutting is started at down-milling 2800 rpm. The nominal plant of the disturbance observer in Fig. 4 is assumed to be a rigid body model of the stage. The proposed

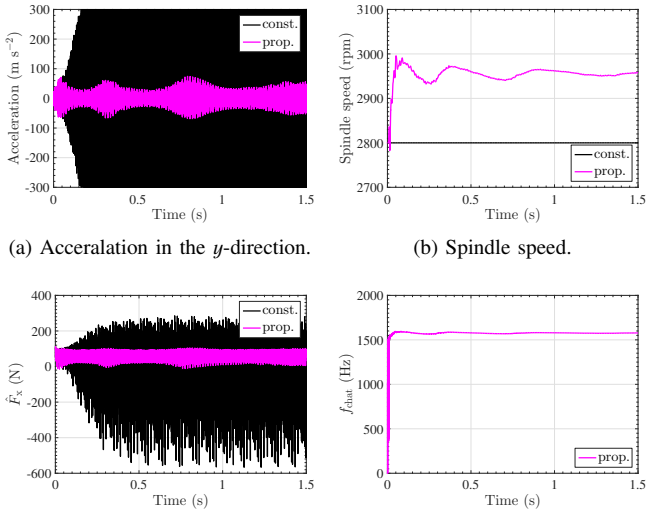


(a) Acceralation in the $y$-direction. (b) Spindle speed.

(c) Estimated Disturbance $\hat{F}_x$. (d) Estimated chatter frequency.

Fig. 6: Simulation results.

method is verified by evaluating the acceleration in the y direction of the tool which is the roughness direction.

The simulation results of constant speed (const.) and proposed method (prop.) are shown in Fig. 6. From Fig. 6a, it is seen that instability occurs when the spindle speed is 2800 rpm. Meanwhile in the proposed method, chatter avoidance starts at 0.01 s as shown in Fig. 6b when the estimated self-excited chatter $\hat{F}_u^2$ exceeds $\sigma_{th}$. In Fig. 6d chatter frequency is estimated as 1570 Hz at 0.1 s and then $\rho_{new}$ is calculated as 8 by (25). From (26), $\omega_{new}$ is calculated as 1570/8/4·60 = 2943 rpm. As shown in Figs. 6a and 6b, the proposed method achieves chatter avoidance by adaptively changing the spindle speed without using external sensors.

## V. Experiment

### A. Experimental setup

The experimental setups are shown in Fig. 7. All cuts have been made in aluminum alloy A6063 using a Mitsubishi Material 4MCD1200 four flutes cutter. Acceleration is measured, only for evaluation, by PCB PIEZOTRONICS A17 accelerometer mounted at the top of the tool. The mechanical parameters in Table Ia are obtained by the hammering test shown in Fig. 8. The stage position is measured by Magnescale LASERSCALE L-55 linear encoder with

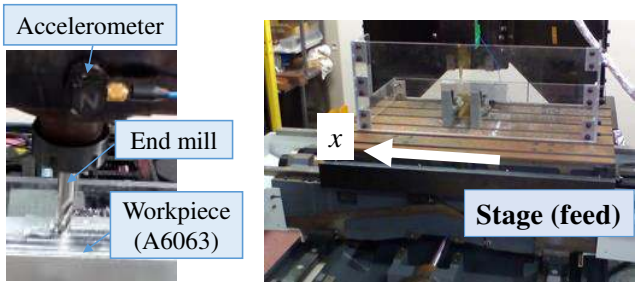


(a) End milling. (b) NC machining table (ball-screw-driven).

Fig. 7: Experimental equipments.

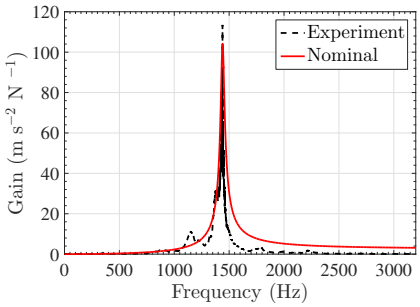


Fig. 8: FRF measurement of the tool by a hammering test and its nominal model $(\boldsymbol{M}s^2 + \boldsymbol{C}s + \boldsymbol{K})^{-1}$.

a resolution of 20 bits. The bandwidths of the stage and the spindle velocity control system, the parameters of the adaptive filter and the machining conditions are same as those in the simulation studies. The proposed method is verified by evaluating the acceleration of the tool in the $y$ direction which is the roughness direction.

### B. Experimental results

The experimental results of constant speed (const.) and proposed method (prop.) are shown in Fig. 10. Chatter avoidance starts at 0.05 s when the estimated self-excited chatter $\hat{F}_u^2$ exceeds the threshold value. The frequency of self-excited chatter is estimated as 1390 Hz at 0.3 s as shown in Fig. 10f. $\rho_{\text{new}} = \text{round}(1390/(2800/60 \cdot 4))$ is calculated as 7 from (25). Therefore, $\omega_{\text{new}}$ is calculated as 1390/7/4·60 = 2980 rpm. Fig. 9 shows the stable spindle speed $\omega_{\text{new}}$.

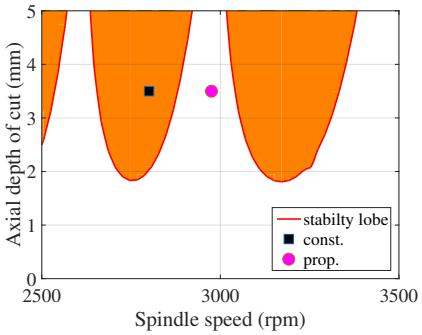


Fig. 9: Cutting condition in the experimental studies in the stability lobe diagram. The "const." and the "prop." represent the initial spindle speed 2800 rpm and $\omega_{\text{new}}$ in a steady state, respectively.

### C. Discussion

Compared to the case of constant speed, the proposed method achieves 60% and 80% improvement in the maximum values in Fig. 10a and in Fig. 10b, respectively. Furthermore in Fig. 11, it is shown that the proposed method achieves 57% and 67% improvement in RMS values and in the maximum values of the frequency component, respectively. Fig. 12 shows the equivalent diagram of the 2DOF milling. Fig. 13 shows the frequency responses of $1 - e^{-\tau s}$ when the spindle speed is 2800 rpm ("const.") and when the spindle speed is adjusted to 2980 rpm ("prop."), respectively. In Fig. 12, it is seen that the regenerative variation of chip thickness $\boldsymbol{h}_{\text{d}}$ is removed when the transfer function $1 - e^{-\tau s}$ is 0. In Fig. 13, it is seen that $1 - e^{-\tau s}$ at the frequency $f_{\text{chat}}$, which is 1390 Hz at 0.3 s, is 0 when the proposed method is applied. Therefore the dominant chatter vibration is eliminated when the proposed method is applied. Hence the proposed method stabilizes machining.

The chatter frequency is estimated as 1390 Hz in Fig. 10f, which corresponds to the result that the peak frequency of $\hat{F}_{\text{u}}$ is 1390 Hz as shown in Fig. 10e. Meanwhile, the peak frequency of the acceleration is 1430 Hz in Fig. 10a, which is different by 40 Hz compared to the estimated value. This difference arises because the disturbance caused by chatter vibration cannot be distinguished from that caused by modeling errors of the stage in DOB [13]. However, as shown in Fig. 9, it is not necessary to strictly select the exact stable speed because the pocket has a certain margin. Therefore even if there are some modeling errors, it is possible to keep stable cutting by the proposed method.

From the above discussion, it is obvious that the proposed method adaptively avoids chatter vibration without external sensors. Therefore, it can be concluded that the proposed method works in practice and guarantees stable machining.

## VI. Conclusion

In this paper, using a high resolution linear encoder, the control method to adaptively estimate and avoid chatter vibration without external sensors were proposed. The proposed method was verified by simulation and experimental studies conducted by the NC end milling.

The proposed method requires the plant model of the stage in order to design the disturbance observer, but meanwhile promises stable machining without chatter vibration while not requiring external sensors. Hence it is expected that the proposed method improves the machining productivity.

## References

[1] Y. Altintas, *Manufacturing automation: metal cutting mechanics, machine tool vibrations, and CNC design*. Cambridge university press, 2012.

[2] Y. Sun and Z. Xiong, "An optimal weighted wavelet packet entropy method with application to real-time chatter detection," *IEEE/ASME Transactions on Mechatronics*, vol. 21, no. 4, pp. 2004–2014, 2016.

[3] Y. Ding, L. Zhu, X. Zhang, and H. Ding, "Stability analysis of milling via the differential quadrature method," *Journal of Manufacturing Science and Engineering*, vol. 135, no. 4, p. 044502, 2013.

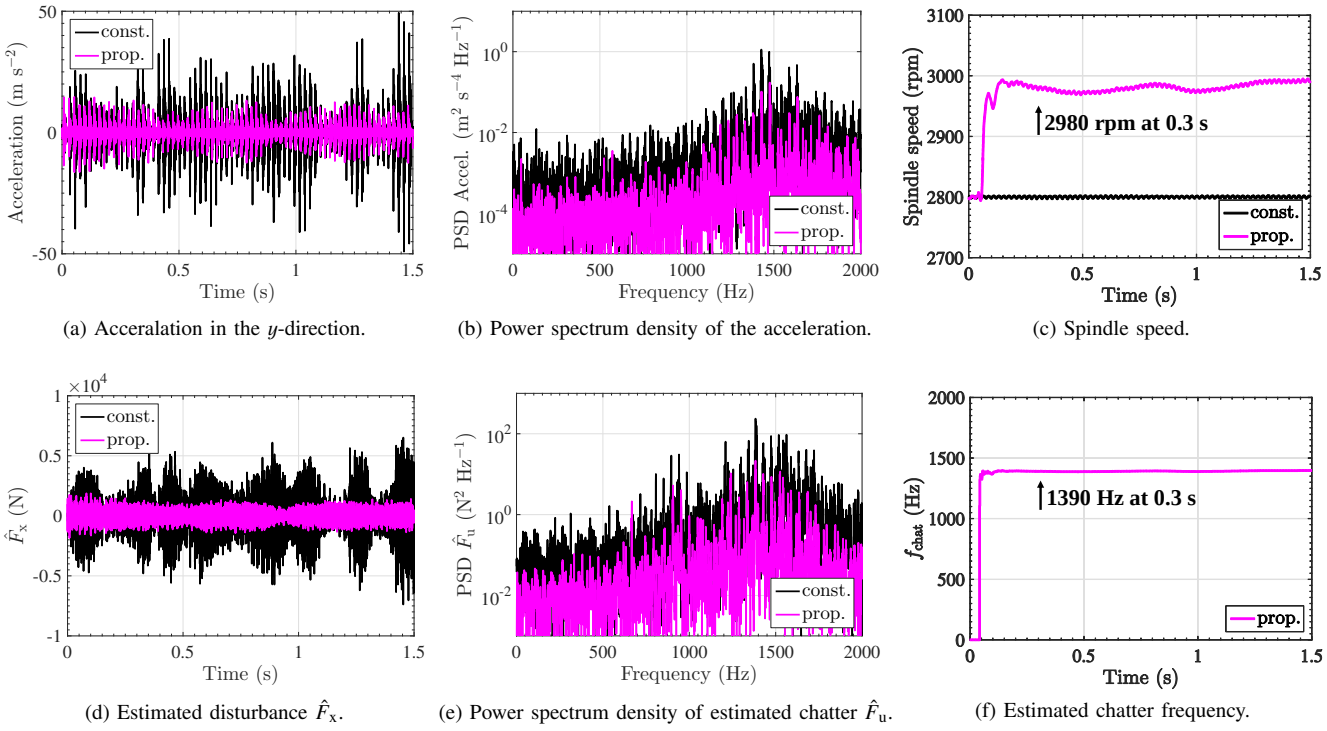


(a) Acceralation in the $y$-direction. (b) Power spectrum density of the acceleration. (c) Spindle speed.

(d) Estimated disturbance $\hat{F}_x$. (e) Power spectrum density of estimated chatter $\hat{F}_u$. (f) Estimated chatter frequency.

Fig. 10: Experimental results.

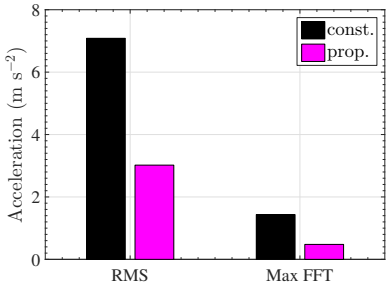


Fig. 11: RMS and maximum values of frequency component (Max FFT) of the acceleration in the experiments.

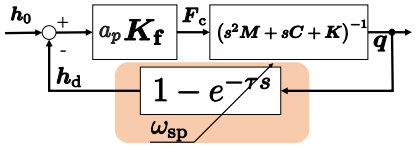


Fig. 12: Block diagram of the 2DOF milling equivalent to that in Fig. 1b.

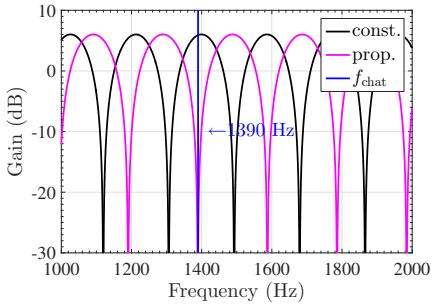


Fig. 13: Frequency response of $1 - e^{-\tau s}$ at 0.3 s in Fig. 10.


[4] T. Insperger and G. Stépán, *Semi-discretization for time-delay systems: stability and engineering applications*, vol. 178. Springer Science & Business Media, 2011.

[5] T. Insperger and G. Stépán, "Updated semi-discretization method for periodic delay-differential equations with discrete delay," *International Journal for Numerical Methods in Engineering*, vol. 61, no. 1, pp. 117–141, 2004.

[6] J. Munoa, X. Beudaert, Z. Dombovari, Y. Altintas, E. Budak, C. Brecher, and G. Stepan, "Chatter suppression techniques in metal cutting," *CIRP Annals-Manufacturing Technology*, vol. 65, no. 2, pp. 785 – 808, 2016.

[7] Y. Kakinuma, Y. Sudo, and T. Aoyama, "Detection of chatter vibration in end milling applying disturbance observer," *CIRP Annals - Manufacturing Technology*, vol. 60, no. 1, pp. 109–112, 2011.

[8] N. Van Dijk, E. Doppenberg, R. Faassen, N. Van de Wouw, J. Oosterling, and H. Nijmeijer, "Automatic in-process chatter avoidance in the high-speed milling process," *Journal of dynamic systems, measurement, and control*, vol. 132, no. 3, pp. 1–14, 2010.

[9] T. Yoneoka, Y. Kakinuma, K. Ohnishi, and T. Aoyama, "Disturbance observer–based in-process detection and suppression of chatter vibration," *Procedia CIRP*, vol. 1, pp. 44–49, 2012.

[10] M. Lamraoui, M. Thomas, M. El Badaoui, and F. Girardin, "Indicators for monitoring chatter in milling based on instantaneous angular speeds," *Mechanical Systems and Signal Processing*, vol. 44, no. 1, pp. 72–85, 2014.

[11] M. F. Corapsiz and K. Erenturk, "Trajectory tracking control and contouring performance of three-dimensional cnc," *IEEE Transactions on Industrial Electronics*, vol. 63, no. 4, pp. 2212–2220, 2016.

[12] S. Zhao and Z. Gao, "An active disturbance rejection based approach to vibration suppression in two-inertia systems," *Asian Journal of Control*, vol. 15, no. 2, pp. 350–362, 2013.

[13] W.-H. Chen, J. Yang, L. Guo, and S. Li, "Disturbance-observer-based control and related methods - an overview," *IEEE Transactions on Industrial Electronics*, vol. 63, no. 2, pp. 1083–1095, 2016.